HARP Collaboration

HARP Memo 04-101
7 May 2004
http://cern.ch/dydak/crosstalk4.ps

Performance of TPC crosstalk correction

F. Dydak, A. Guskov, A. Krasnoperov, Yu. Nefedov, J. Wotschack, A. Zhemchugov

Abstract

The performance of the CERN-Dubna-Milano (CDM) algorithm for TPC crosstalk correction is presented. The algorithm is designed to correct for uni-directional and bi-directional crosstalk, but not for self-crosstalk. It reduces at the 10% level the number of clusters, and the number of pads with a signal above threshold. Despite of dramatic effects in selected channels with complicated crosstalk patterns, the average longitudinal signal shape of a hit, and the average transverse signal shape of a cluster, are little affected by uni-directional and bi-directional crosstalk. The longitudinal signal shape of hits is understood in terms of preamplifier response, longitudinal diffusion, track inclination, and self-crosstalk. The transverse signal shape of clusters is understood in terms of the TPC's pad response function. The CDM crosstalk correction leads to an average charge decrease at the level of 15%, though with significant differences between TPC sectors. On the whole, crosstalk constitutes a relatively benign malfunction of the TPC readout which, after correction by the CDM algorithm and with proper attention to self-crosstalk, is not an obstacle to progress with physics analysis.

1 Introduction

The CERN-Dubna-Milano (CDM) algorithm for TPC crosstalk correction is a data-driven, model-independent approach to the problem of crosstalk correction. It accounts for arbitrary amplitudes and pulse shapes of signals, and corrects (almost) all generations of uni-directional and bi-directional crosstalk, with a view to handling (almost) correctly even complex multi-track events. It is not, however, designed to correct for self-crosstalk as such correction is deemed unnecessary.

The categories of uni-directional, bi-directional and self-crosstalk are amply discussed in an earlier memo [1]. The correction algorithm for uni-directional and bi-directional crosstalk was originally developed by two of us (A. G. and A. Z.), and is described in detail in this earlier memo. The algorithm has not changed since its internal publication in mid 2003, and is since that time routinely applied in diverse studies of TPC characteristics.

In general, the three categories of crosstalk can exist on top of each other. Crosstalk can produce quite dramatic effects in selected channels, as shown in Ref. [1]. Therefore, one would require any crosstalk correction algorithm to achieve the following:

- in **individual** events taken during the test-charge injection campaign of V. Serdyuk (for details, see Ref. [1]), the ADC signals in all satellite pads must vanish; however, this is a necessary condition only; it is not sufficient *per se* to demonstrate the validity of the algorithm; it merely proves the algorithm's internal consistency and it gives some reassurance that the software code is free of major bugs;
- after correction, the **longitudinal** signal shape of a 'hit', i.e. the series of contiguous charge-samplings in 100 ns intervals within a given pad, must be compatible with the pulseshape expectation from preamplifier response, longitudinal diffusion, track inclination and self-crosstalk;
- after correction, the **transverse** signal shape of a 'cluster', i.e. the distribution of time-integrated ADC signals over contiguous pads in the same pad row, must be compatible with the TPC's pad response function.

Of the above three requirements, the first has been shown already to be met in the earlier memo on the CDM crosstalk algorithm [1] and needs not be discussed again. Rather, we concentrate in this paper on the longitudinal signal shape of a hit (Section 2), and on the transverse signal shape of a cluster (Section 3).

Hits and clusters along both physics and cosmic-muon tracks are used to illustrate the performance of the CDM algorithm.

We wish to recall that the CDM algorithm, which is the first step in the series of software operations on the TPC data, acts on the response of pads **before** the equalization of their responses. Therefore, signals both before and after the crosstalk correction are *a priori* expected to be discussed in terms of **ADC counts** and not in terms of **equalized charges**.

However, we consider the performance of the crosstalk correction in terms of equalized charges closer to physics analysis issues. Accordingly, all results presented in this paper unless otherwise stated, have the pad equalization constants from the analysis of krypton decay events applied [2]. Thus all pads can be regarded as delivering, within about 5%, the same amplified charge for the same primary charge deposit in the TPC gas.

We wish to stress that the feature of the CDM algorithm of correcting for uni-directional and bi-directional crosstalk, but not for self-crosstalk, renders all our subsequent software operations on the TPC data, including the validity of respective calibration constants, dependent on the prior application of the CDM algorithm.

2 Longitudinal signal shape of a hit

The longitudinal signal shape of a hit is first of all determined by the convolution of three effects (the small effect of different path lengths of electrons drifting to the same sense wire is neglected):

1. the **longitudinal diffusion** which causes a jitter in the arrival of the primary electrons at the sense wires;
2. the **electronics response** of the preamplifier which is asymmetric in time (the rise is faster than the fall); and
3. the **inclination of the track** with respect to the pad plane, in conjunction with the relatively large radial size of ~ 16 mm of a TPC pad.

There is an important fourth effect, though: **self-crosstalk** lengthens the longitudinal signal shape.

The longitudinal diffusion increases with the square root of the driftlength. It is approximated by a Gaussian with an RMS of ~ 4 mm $\cong 80$ ns at 1 m driftlength, suitable for the TPC gas of 91% argon and 9% methane at atmospheric pressure [3].

The preamplifier response to a δ-charge input is approximated by the function [4]

$$f(t) = t^2 \exp(-t/100) ,$$

where t is the time in ns.

Especially for very forward- or very backward-going tracks, i.e. tracks with very small or very large polar angle, the geometrical effect of track inclination with respect to the pad plane constitutes an important contribution to the longitudinal signal shape.

We show in Fig. 1 what we expect from the convolution of the above three effects, for straight tracks from a target at $z = 0$. The upper plot shows longitudinal signal shapes from transverse tracks with polar angles between 64 and 116° (FWHM ~ 370 ns), the lower plot shows the same for forward tracks with polar angles between 18° and and 64° (FWHM ~ 500 ns). The plots show the pulse shapes **before sampling, digitization and pedestal subtraction, and without lengthening due to self-crosstalk**. While these pulse shapes are to be understood as **qualitative** only (self-crosstalk is accepted as an experimental fact; there is no necessity to model it theoretically), they underline the expectation that pulses from forward-going tracks are longer than pulses from transverse tracks.

2.1 Longitudinal hit profile of transverse tracks

In Fig. 2 we show the **average** longitudinal charge profile of a single hit, before and after the crosstalk correction, for transverse tracks in physics data (+8.9 GeV/c, 5% Be target) with polar angles between 64° and 116° (this ensemble of tracks is expected to be dominated by tracks with a polar angle close to 64°). In Figs. 3 and 4 we show the same but separately for the sectors 1 to 6.

These plots as well as subsequent analogous plots in this Section are normalized to a single hit. On the one hand, since the number of hits is reduced by the crosstalk correction, this normalization will **increase** the charge per hit. On the other hand, the crosstalk correction *per se* **reduces** the charge per hit. The signal shape after crosstalk correction shows the net result of these two adverse effects.

In order to appreciate the relative size of the signals between TPC sectors, and between physics and cosmic-muon tracks, all plots of the same quantity use the same ordinate scale.

The main conclusion is that the average change of the charge due to the crosstalk correction is not large, although the crosstalk correction is largest for tracks in the transverse direction. The longitudinal pulseshape is satisfactorily regular, even before crosstalk correction (notwithstanding the fact that in specific events there is quite some longitudinal re-shuffling of charges by the crosstalk correction). The main signal characteristics are the FWHM which is $\sim$ 400 ns. The six TPC sectors have comparable signal shapes.

The signal shapes show the average over **all** pads involved, i.e. over pads with self-crosstalk, and pads without self-crosstalk.

Figure 5 shows the action of the crosstalk correction algorithm in four selected pads with a larger than average charge reduction. While the two lower plots show the normal signal shape, the two upper plots show typical signal shapes when self-crosstalk is at work. It is important to note that (i) the correction algorithm leaves self-crosstalk intact, while both the integral as well as the longitudinal shape can be altered by the correction for uni-directional and bi-directional crosstalk, and (ii) different categories of crosstalk can exist on top of each other.

To highlight the importance of self-crosstalk, Fig. 6 shows the longitudinal signal shape of four selected pads after crosstalk correction. The two left plots show the normal signal shape, while the signal shapes in the right two plots are about doubled in length due to self-crosstalk. In terms of millimetres of drift distance, this amounts to $\sim$ 4 cm FWHM instead of $\sim$ 2 cm. Another feature is that small pulseheights in the tail of pulses are not perfectly eliminated which is a direct consequence of imperfections of the pedestal subtraction at the time of data taking. Obviously, both effects require special precautions in the algorihm which determines the cluster's z position. This will be quantitatively addressed, *inter alia*, in a forthcoming memo [5].

Table 1 summarizes for transverse physics tracks the reduction in the number of pads and clusters, as well as the average reduction of the charge of a hit, separately for all TPC sectors and for the whole TPC. The number of clusters decreases in general, however this is not a necessity, as the clustering algorithm deals with a different situation after the crosstalk correction.

Firstly, we note that different sectors have different average crosstalk corrections.

While the reduction in the number of pads is $\sim 16\%$, the reduction in the number of clusters is $\sim 5\%$. Hence the crosstalk correction removes mainly pads (single or part of clusters), and less often clusters.

The reduction of the average time-integrated charge of a hit is $\sim 24\%$. This charge reduction of a hit is normalized to the same number of events (3000) before and after the crosstalk correction.

Table 1: Characteristics of the crosstalk correction for transverse physics tracks.

	No.pads	No.clusters	No.pads	No.clusters	charge decrease
	Before correction		After correction		%
sector 1	5878	2114	4917	2012	23.2
sector 2	4827	1928	4336	1934	17.4
sector 3	6607	2340	5669	2240	23.9
sector 4	7138	2595	5546	2295	32.6
sector 5	6746	2635	5420	2418	27.2
sector 6	6180	2215	5501	2183	13.5
all	37376	13827	31389	13082	23.5

Figure 7 shows the **average** longitudinal charge profile of a single hit before and after the crosstalk correction, for transverse cosmic-muon tracks with polar angles between 64° and 116°. There is no difference to what is seen in physics tracks, except that the average charge of cosmic-muon tracks is noticeably lower than the one of physics tracks.

2.2 Longitudinal hit profile of forward tracks

In Fig. 8 we show the **average** longitudinal charge profile of a single hit before and after the crosstalk correction, for forward physics tracks with polar angles between 18° and 64° (this ensemble of tracks is expected to be dominated by tracks with a polar angle close to 18°).

Figure 9 shows the same as Fig. 8 but on a logarithmic scale. This plot illustrates the longitudinal re-shuffling of charges by the crosstalk correction. It also demonstrates that the crosstalk correction leads to a more regular longitudinal shape.

In Figs. 10 and 11 we show the same as in Fig. 8, but separately for the sectors 1 to 6.

Table 2 summarizes for forward physics tracks the reduction in the number of pads and clusters, as well as the average reduction of the charge of a hit, separately for all TPC sectors and for the whole TPC. We note again that different sectors have different average crosstalk corrections.

While the reduction in the number of pads is $\sim 11\%$, the reduction in the number of clusters is $\sim 2\%$. As expected, these figures are lower than for transverse tracks.

The reduction of the average time-integrated charge of a hit is $\sim 7\%$. Also here, this charge reduction is normalized to the same number of events (3000) before and after the crosstalk correction.

Table 2: Characteristics of the crosstalk correction for forward physics tracks.

	No.pads	No.clusters	No.pads	No.clusters	charge decrease
	Before correction		After correction		%
sector 1	18246	6950	15979	6673	9.3
sector 2	15194	6278	13373	6212	12.9
sector 3	16694	6067	15473	6200	2.3
sector 4	17913	6741	16048	6544	2.1
sector 5	13415	5432	11760	5344	8.2
sector 6	15027	5758	13313	5631	8.1
all	96489	37226	85946	36604	7.1

Figure 12 shows the **average** longitudinal charge profile of a single hit before and after the crosstalk correction, for forward cosmic-muon tracks with polar angles between 18° and 64° (this ensemble of tracks is expected to be dominated by tracks with a polar angle close to 64°). There is again no difference to what is seen in physics tracks, except that the average charge of cosmic-muon tracks is lower than the one of physics tracks.

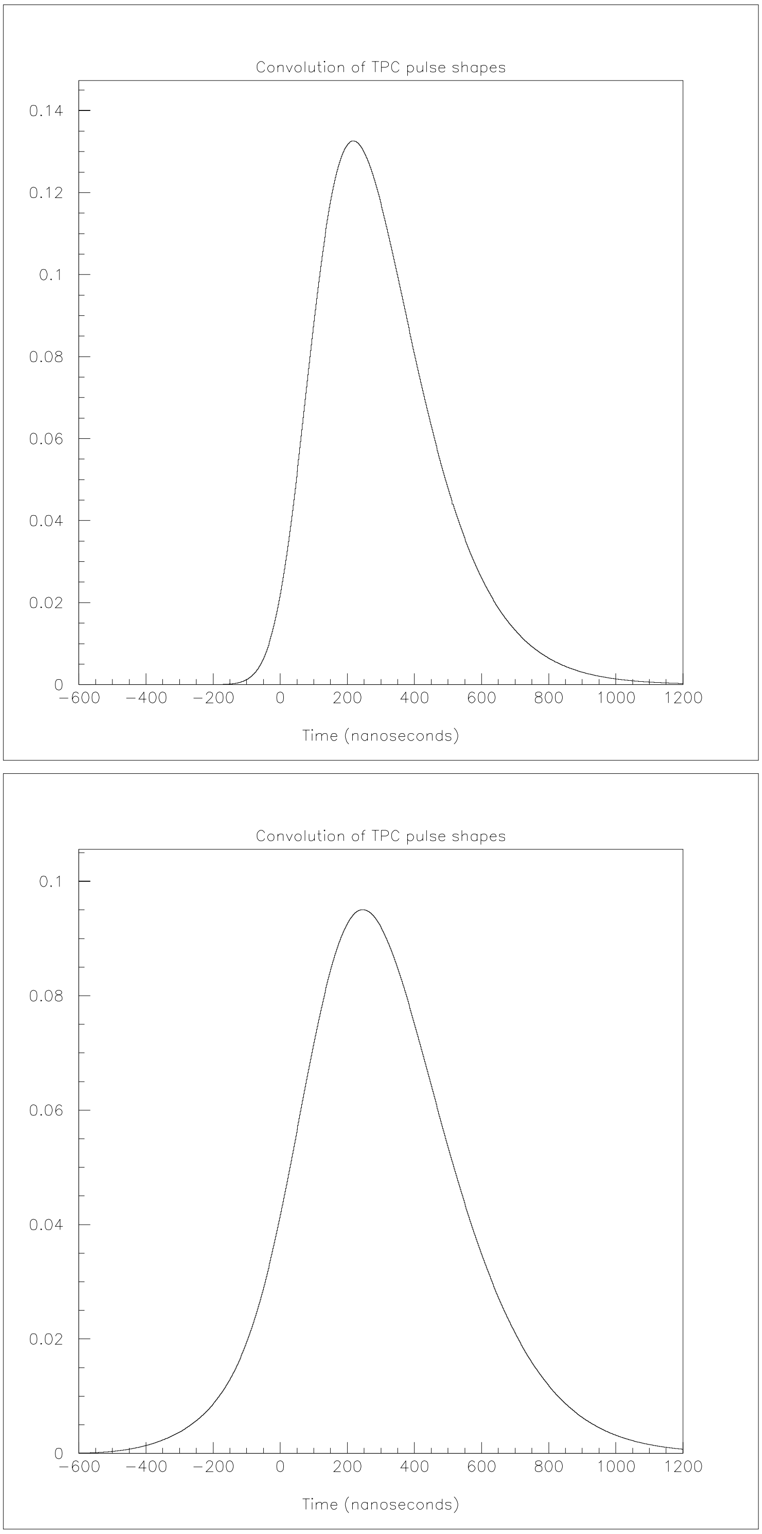

Figure 1: Longitudinal TPC signal shapes before sampling, digitization and pedestal subtraction, and without lengthening due to self-crosstalk, for straight tracks in the transverse (top) and forward (bottom) directions.

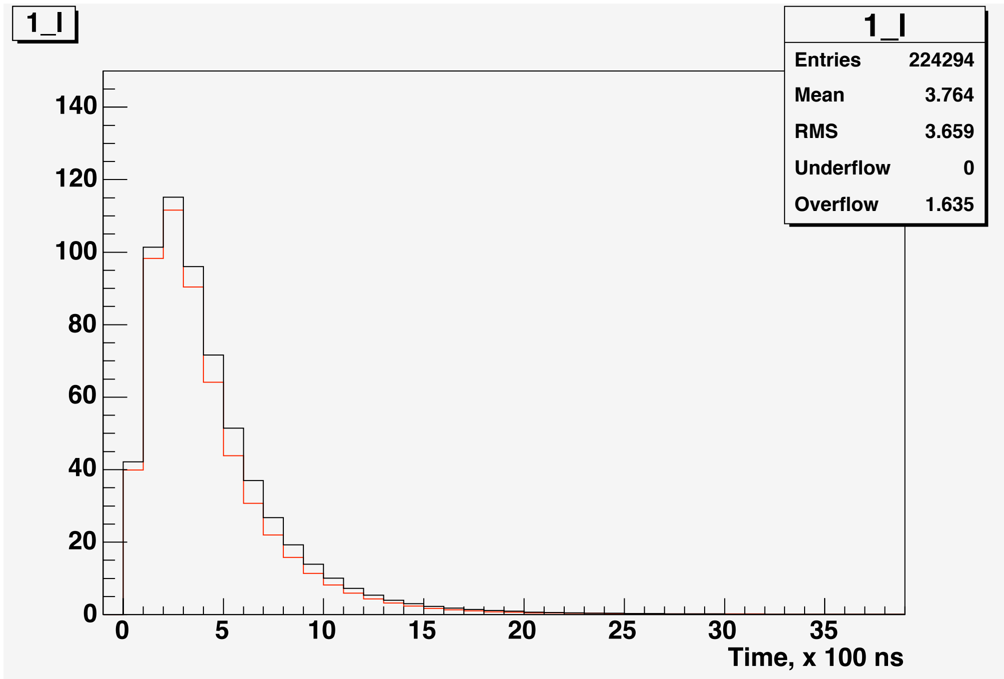

Figure 2: Average longitudinal charge profile of a single hit in transverse physics tracks, before (thick/black) and after (thin/red) correction for crosstalk, for all TPC sectors.

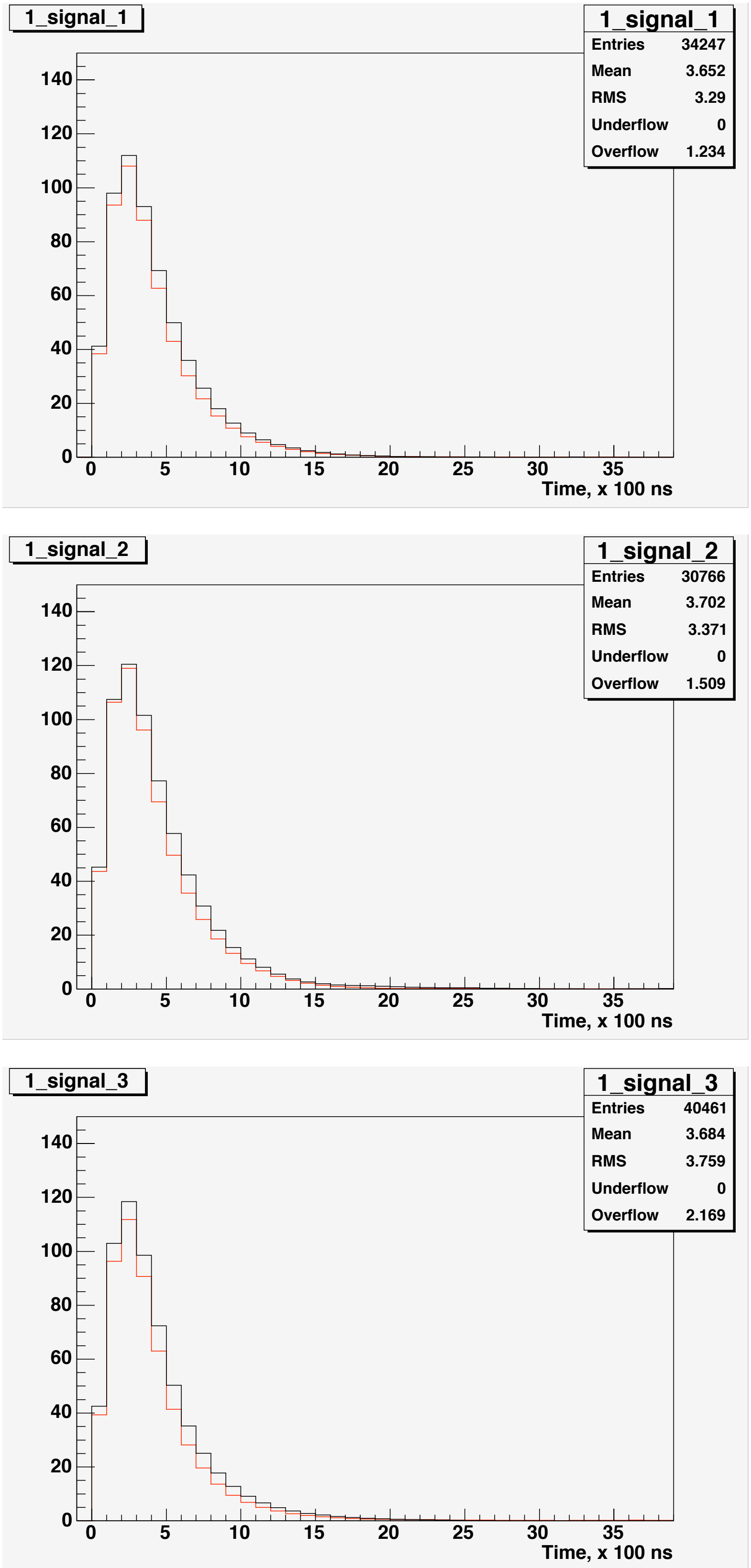

Figure 3: Average longitudinal charge profile of a single hit in transverse physics tracks, before (thick/black) and after (thin/red) correction for crosstalk, for TPC sectors 1 to 3.

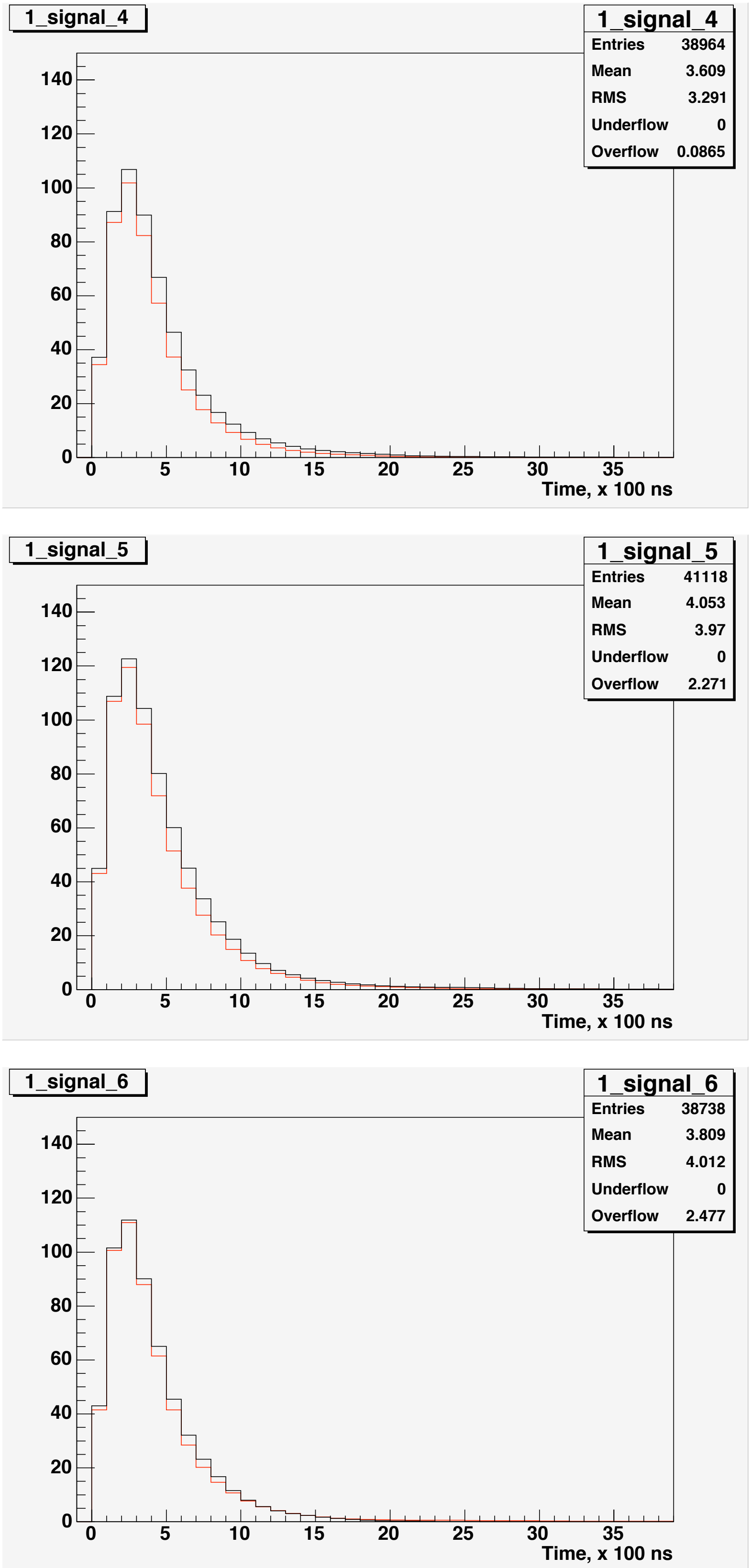

Figure 4: Average longitudinal charge profile of a single hit in transverse physics tracks, before (thick/black) and after (thin/red) correction for crosstalk, for TPC sectors 4 to 6.

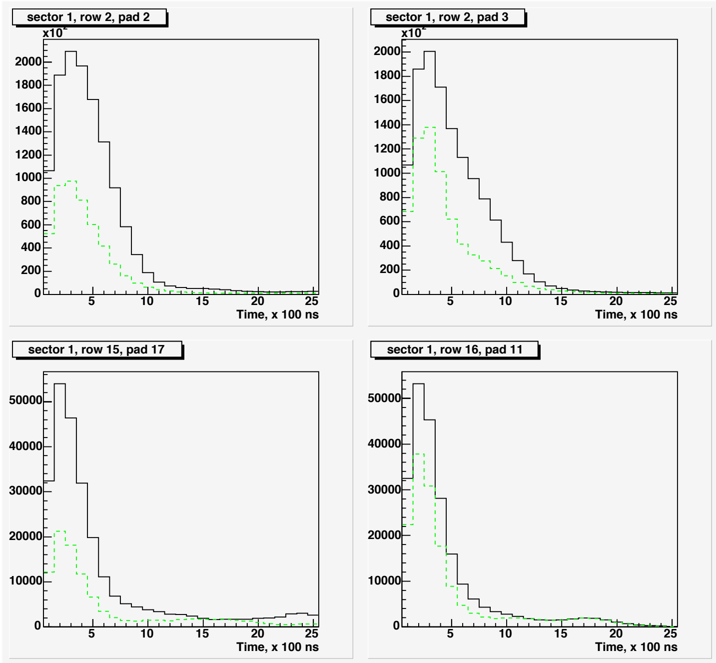

Figure 5: Longitudinal signal shape, in terms of ADC counts, in four selected pads before (full line/black) and after (broken line/green) the crosstalk correction.

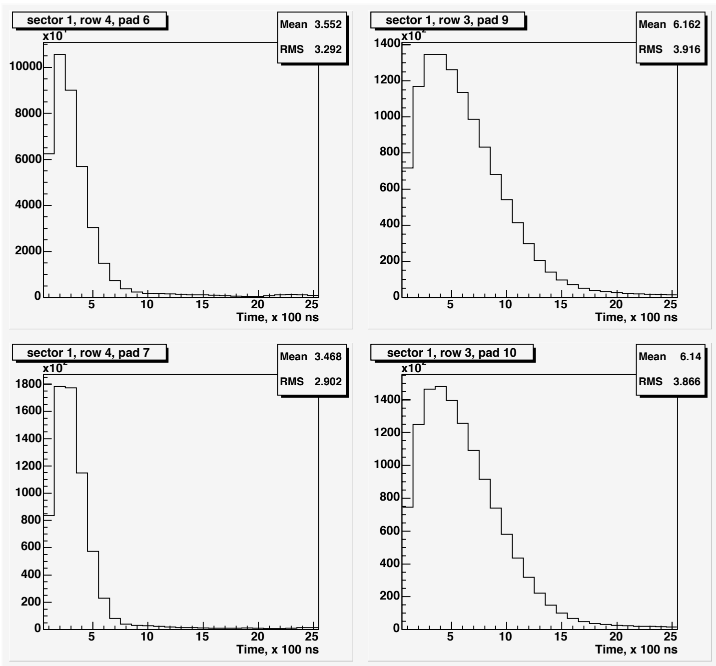

Figure 6: Longitudinal signal shapes, in terms of ADC counts, of four selected pads after crosstalk correction. The signals on the left are normal while the signals on the right show the typical effect of self-crosstalk.

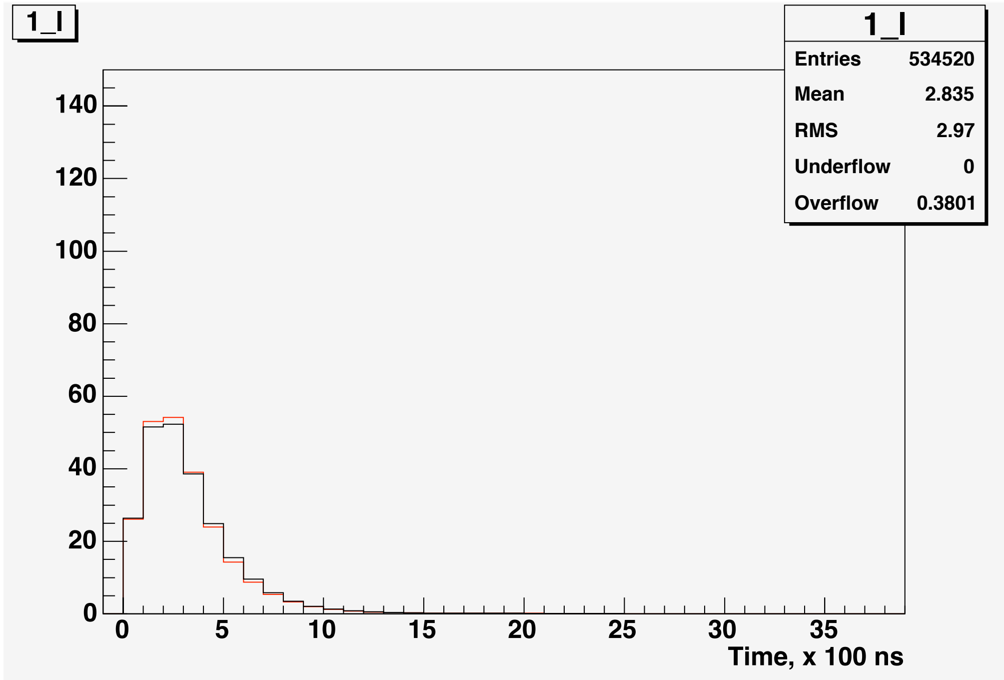

Figure 7: Average longitudinal charge profile of a single hit in transverse cosmic-muon tracks, before (thick/black) and after (thin/red) correction for crosstalk, for all TPC sectors.

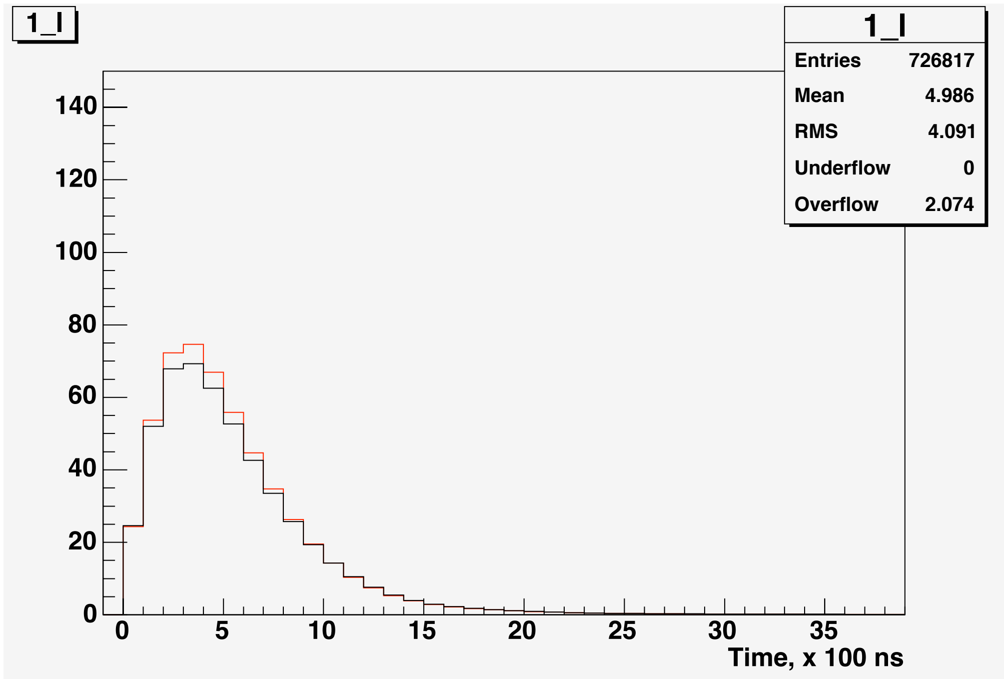

Figure 8: Average longitudinal charge profile of a single hit in forward physics tracks, before (thick/black) and after (thin/red) correction for crosstalk, for all TPC sectors.

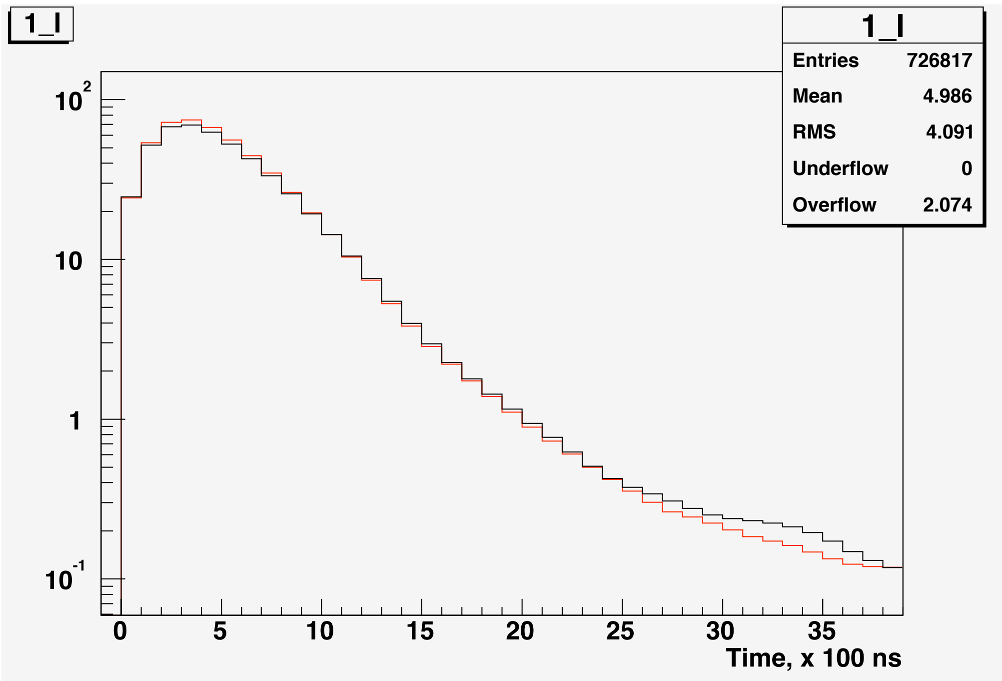

Figure 9: Same as Fig. 8, but on a logarithmic scale.

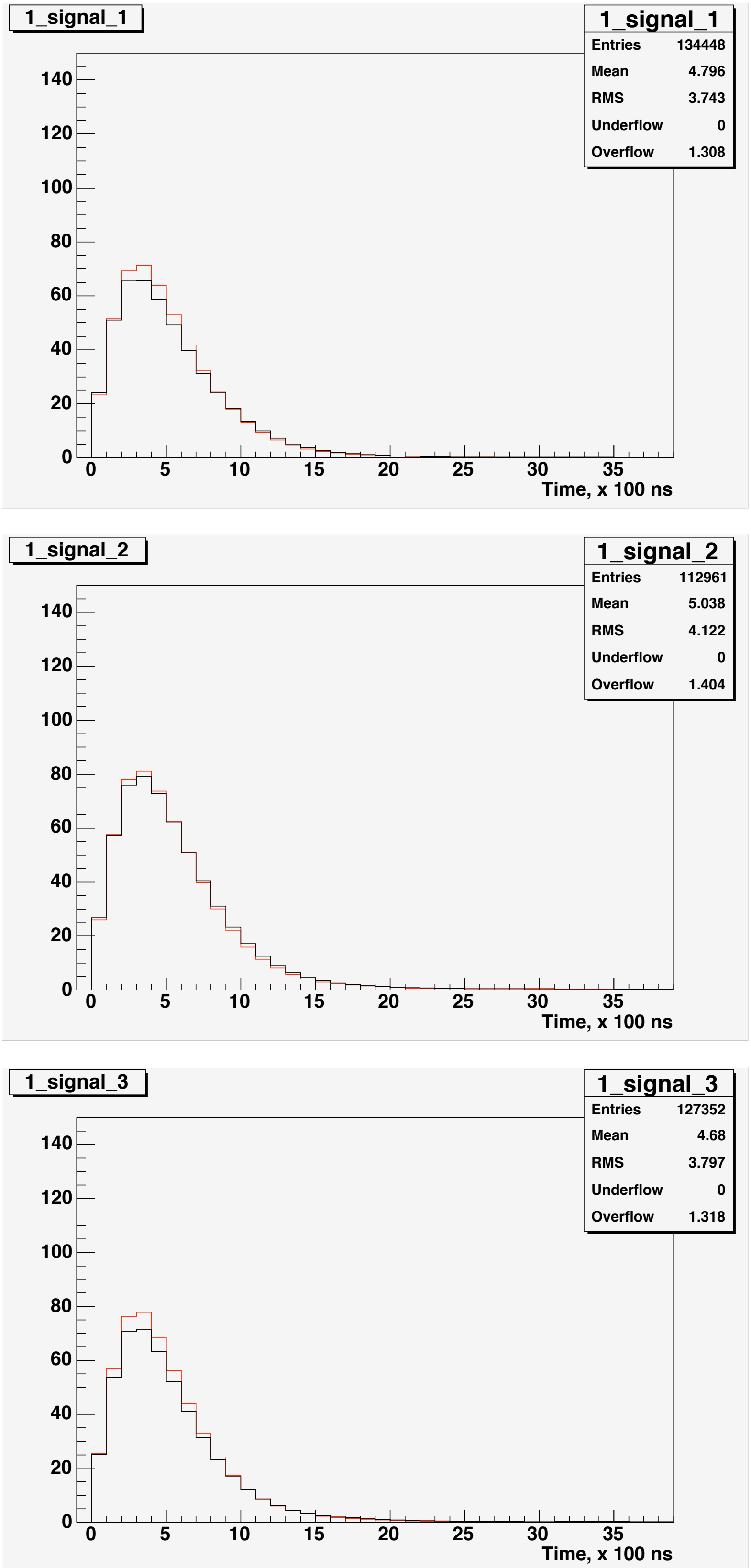

Figure 10: Average longitudinal charge profile of a single hit in forward physics tracks, before (thick/black) and after (thin/red) correction for crosstalk, for TPC sectors 1 to 3.

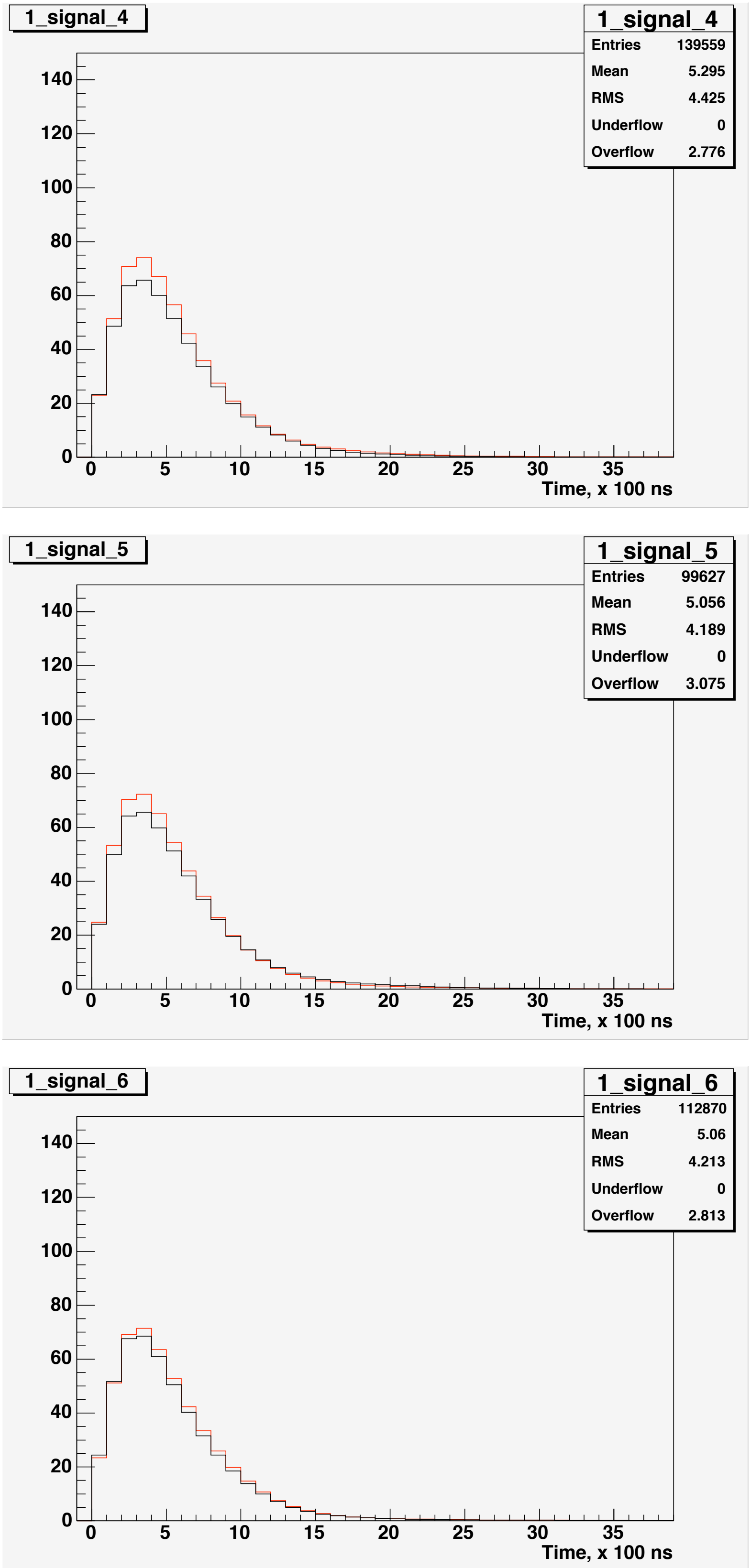

Figure 11: Average longitudinal charge profile of a single hit in forward physics tracks, before (thick/black) and after (thin/red) correction for crosstalk, for TPC sectors 4 to 6.

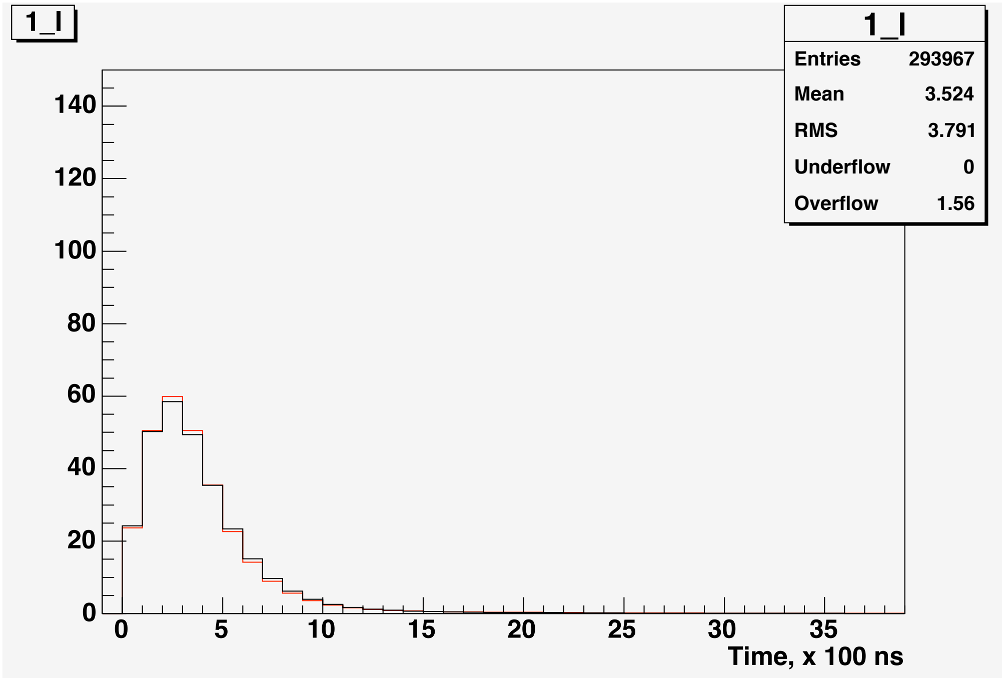

Figure 12: Average longitudinal charge profile of a single hit in forward cosmic-muon tracks, before (thick/black) and after (thin/red) correction for crosstalk, for all TPC sectors.

3 Transverse signal shape of a cluster

The signal measured in the TPC pads is the charge which is generated by influence from the net charge at the sense wires. The 4 mm distance between the pads and the sense wires determines, in first approximation, the spatial distribution of the influenced charge. Further contributions to the lateral distribution arise from (i) transverse charge diffusion in the active volume of the TPC (which is, however, strongly reduced due to the focusing from the $\omega\tau$-effect), (ii) the distance between sense wires, (iii) the distance between sense wires and the ground plane which is opposite to the pad plane, and (iv) the time characteristics of the preamplifier response [6]. Useful parametrizations and Gaussian approximations of the pad response function have been proposed in the literature, e.g. the Gatti–Gordon–Mathieson parametrization [7]. The latter has been used by R. Veenhof to demonstrate that the pad response function measured with the HARP TPCino is in accordance with expectations (see Fig. 13). The TPCino geometry is consistent with a Gaussian $\sigma \cong 3.7$ mm. In the real TPC, one does not measure this pad response function, but an 'effective pad response function' which is obtained in the following way: in a cluster, the pad with the largest signal is defined as central pad out of five, and the 3rd bin of a 5-bin histogram is filled accordingly. The four other bins are filled with the charges of the remaining two pads left and right of the central pad. This procedure is equivalent to a convolution of the pad response function with the 6.5 mm width of the pads, and increases the Gaussian σ from 3.7 mm to 4.1 mm.

In practice, $\sigma = 4.1$ mm must be considered as a lower limit, since the transverse diffusion in the TPC gas and imperfections in the equalization of the response of the preamplifiers of different pads are not taken into account. Altogether, a σ of the effective pad response function between 4 mm and 5 mm appears reasonable.

3.1 Transverse cluster profile of transverse tracks

In Fig. 14 we show the **average** transverse charge profile of a single cluster before and after the crosstalk correction, for transverse physics tracks with polar angles between 64° and 116°. In Figs. 15 and 16 we show the same but separately for the sectors 1 to 6.

These plots as well as subsequent analogous plots in this Section are normalized to a single cluster (note that the number of clusters is normally reduced by the crosstalk correction). All fit results displayed in the plots refer to the distributions after the crosstalk correction.

The shape of the 'effective' pad response function agrees with expectation. The Gaussian σ from a fit to the charge profile of the three central pads after crosstalk correction is consistent with the lower limit of 4.1 mm. Even before the crosstalk correction, the charge profile does not look much different. The uniformity between TPC sectors is satisfactory.

Notwithstanding the close similarity of the transverse charge profiles before and after the crosstalk correction, in individual events the effect can be large. Therefore, the crosstalk correction is expected to reduce the dispersion of the $r \cdot \phi$ coordinate of clusters. This will be quantitatively addressed, *inter alia*, in a forthcoming memo [5].

Figure 17 shows the **average** transverse charge profile of a single cluster before and after

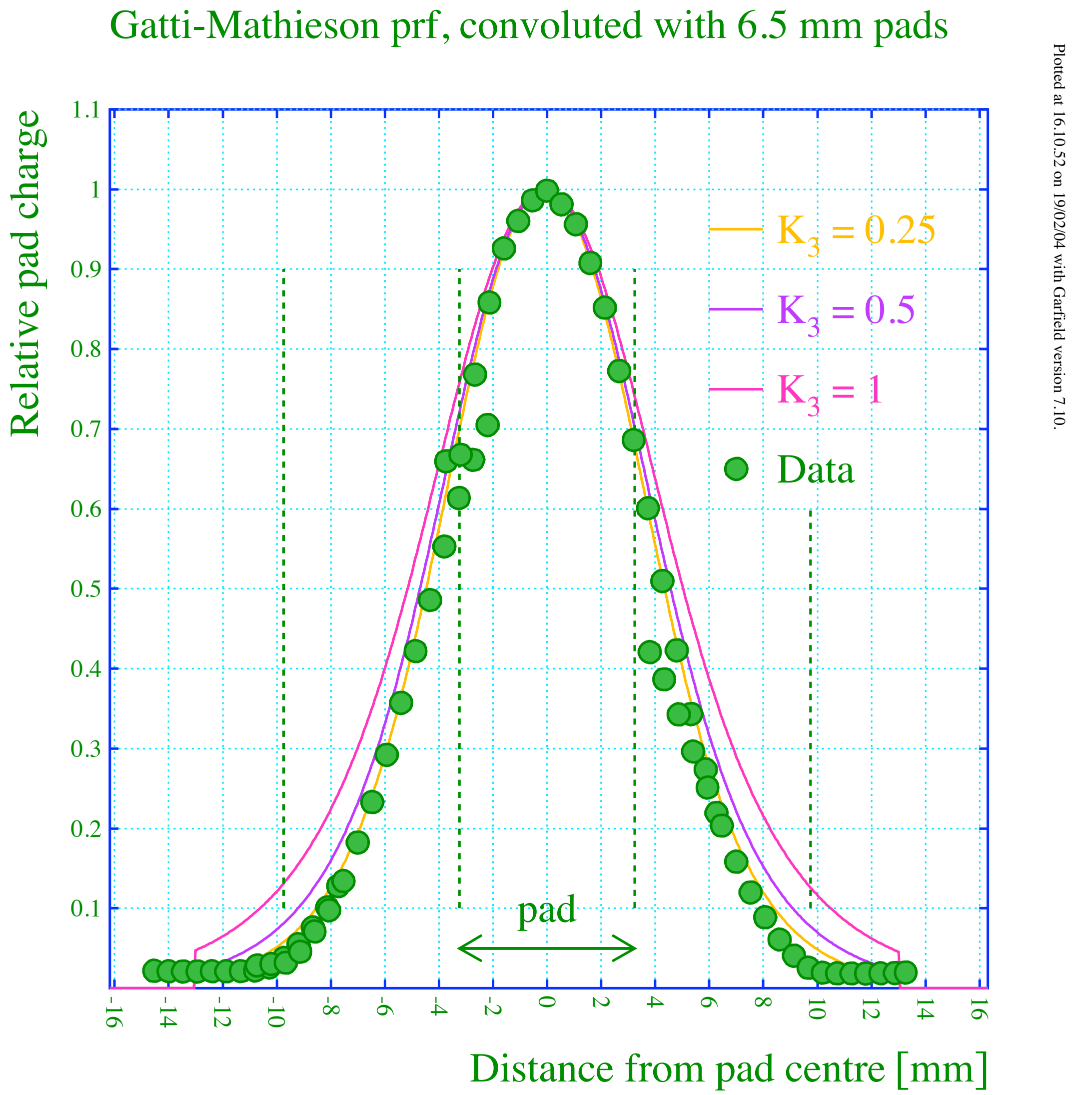

Figure 13: Measured charge response of a pad in the TPCino, as a function of the displacement of the pad centre with respect to the sense wire; the full lines are Gatti-Mathieson parametrizations for the approximate TPCino geometry.

the crosstalk correction, for transverse cosmic-muon tracks with polar angles between 64° and 116°. Again no difference is seen in comparison with physics tracks, except the lower average charge of cosmic-muon tracks.

3.2 Transverse cluster profile of forward tracks

In Fig. 18 we show the **average** transverse charge profile of a single cluster before and after the crosstalk correction, for forward physics tracks with polar angles between 18° and 64°. In Figs. 19 and 20 we show the same but separately for the sectors 1 to 6. All plots demonstrate satisfactory performance.

Figure 21 shows the **average** transverse charge profile of a single cluster before and after the

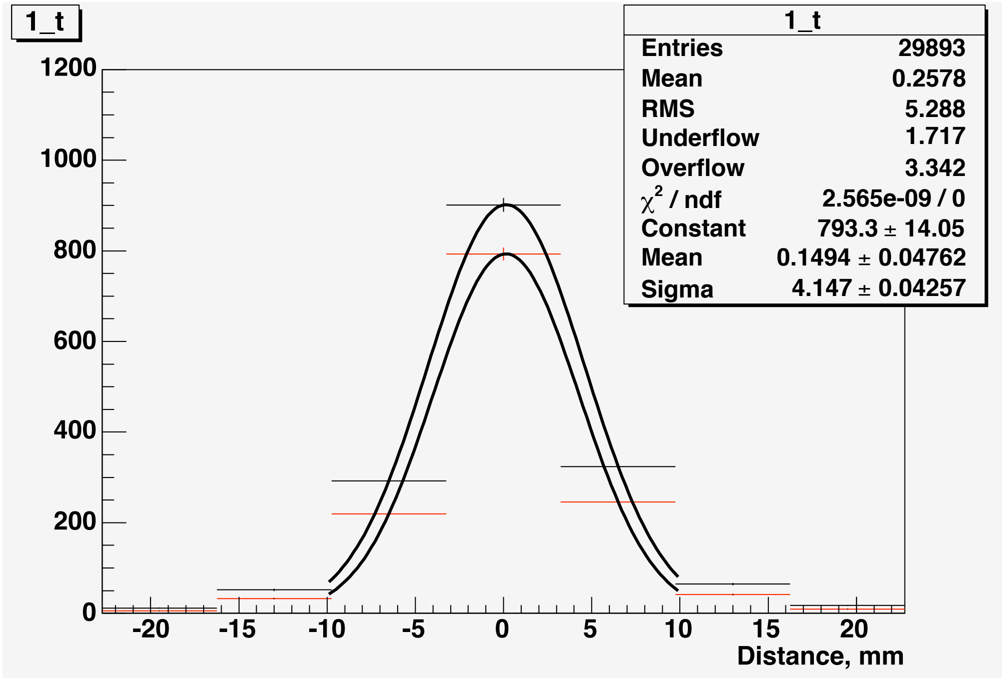

Figure 14: Average transverse charge profile of a single cluster in transverse physics tracks, before (thick/black horizontal bars) and after (thin/red horizontal bars) correction for crosstalk, for all TPC sectors.

crosstalk correction, for forward cosmic-muon tracks with polar angles between 18° and 64°. No difference is seen in comparison with physics tracks, except the lower average charge of cosmic-muon tracks.

4 Summary

The CDM algorithm for TPC crosstalk correction is designed to deal with uni-directional and bi-directional crosstalk, but not with self-crosstalk. It leads to an average charge decrease of order 15%, larger for transverse tracks and smaller for forward tracks, as expected. The average charge decrease differs significantly between TPC sectors. Despite of dramatic effects in selected channels with complicated crosstalk patterns, the crosstalk constitutes on the whole a relatively benign malfunction of the TPC readout, which is satisfactorily taken care of by the CDM algorithm. If proper attention is paid to effects arising from self-crosstalk, TPC crosstalk is not an obstacle to progress with physics analysis.

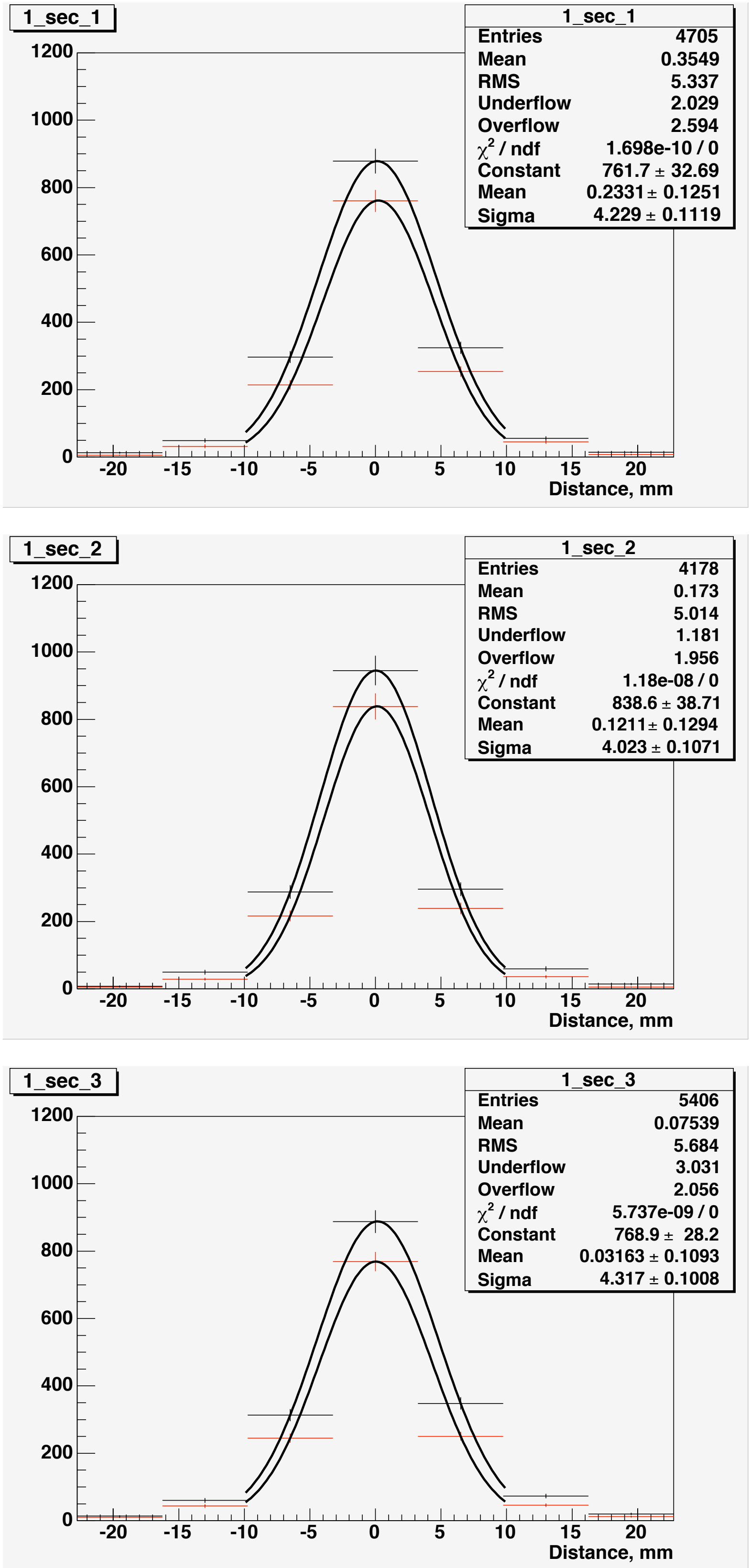

Figure 15: Average transverse charge profile of a single cluster in transverse physics tracks, before (thick/black horizontal bars) and after (thin/red horizontal bars) correction for crosstalk, for TPC sectors 1 to 3.

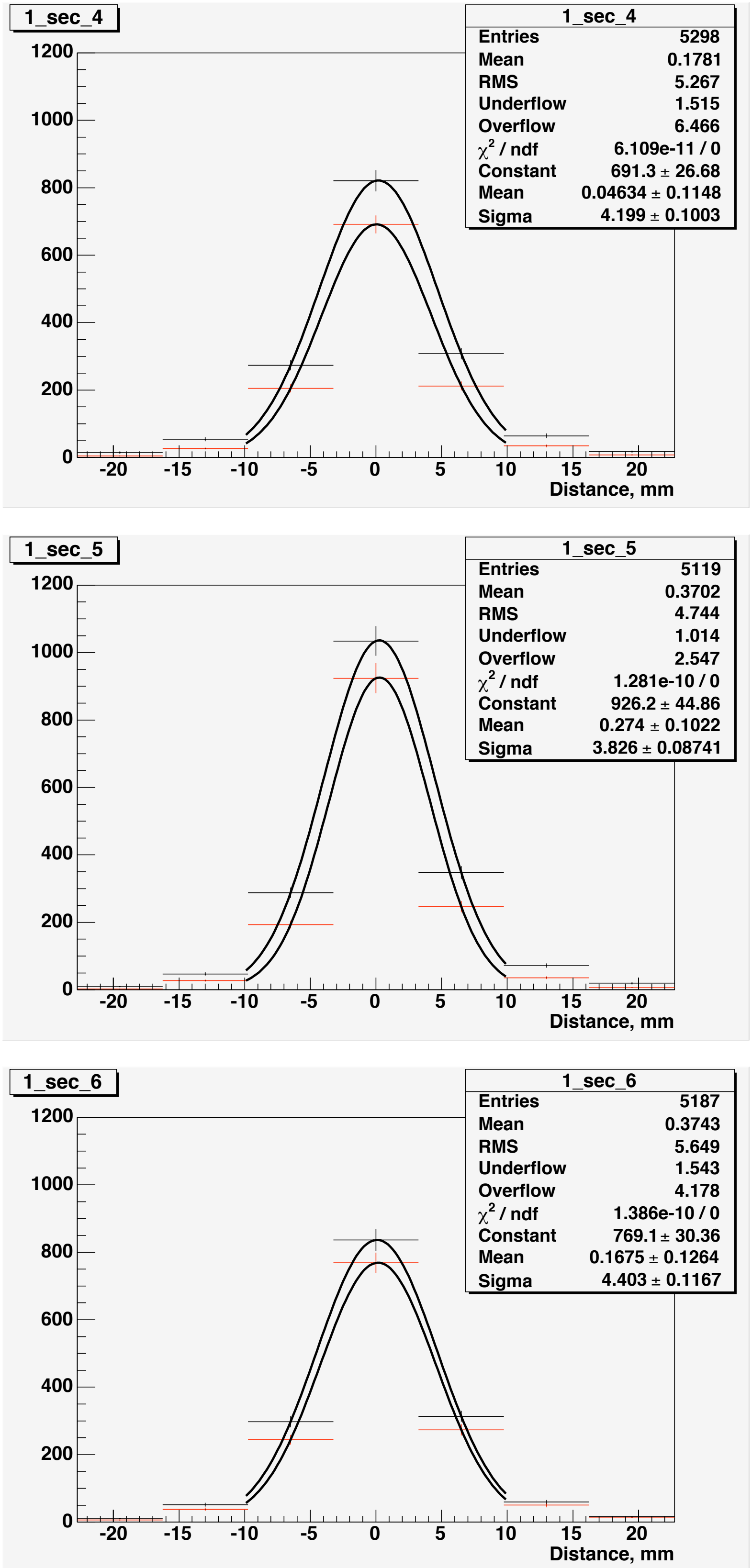

Figure 16: Average transverse charge profile of a single cluster in transverse physics tracks, before (thick/black horizontal bars) and after (thin/red horizontal bars) correction for crosstalk, for TPC sectors 4 to 6.

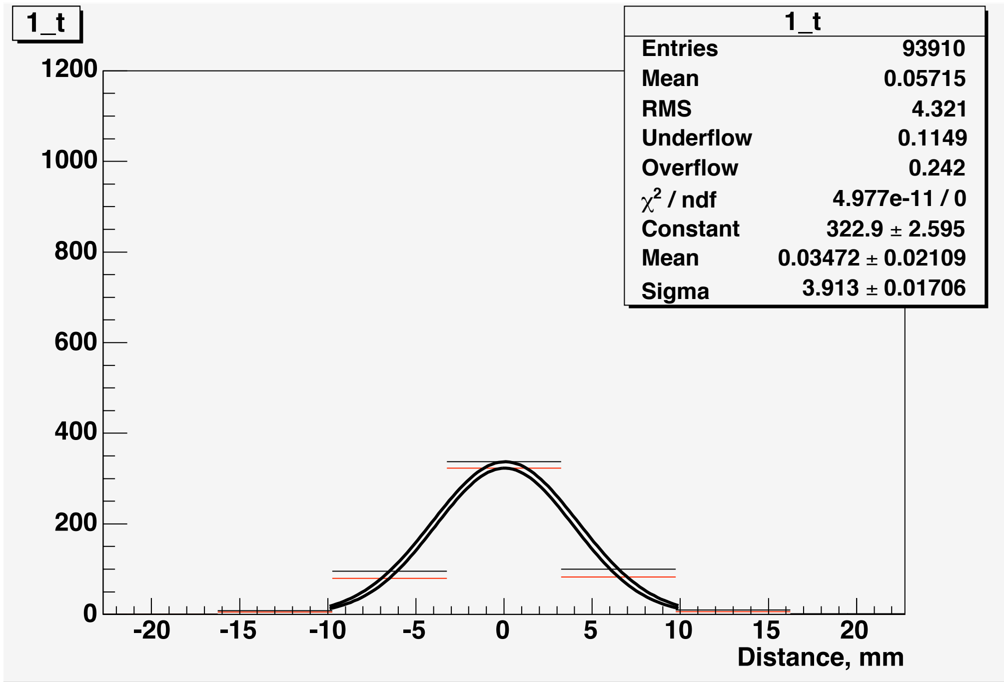

Figure 17: Average transverse charge profile of a single cluster in transverse cosmic-muon tracks, before (thick/black horizontal bars) and after (thin/red horizontal bars) correction for crosstalk, for all TPC sectors.

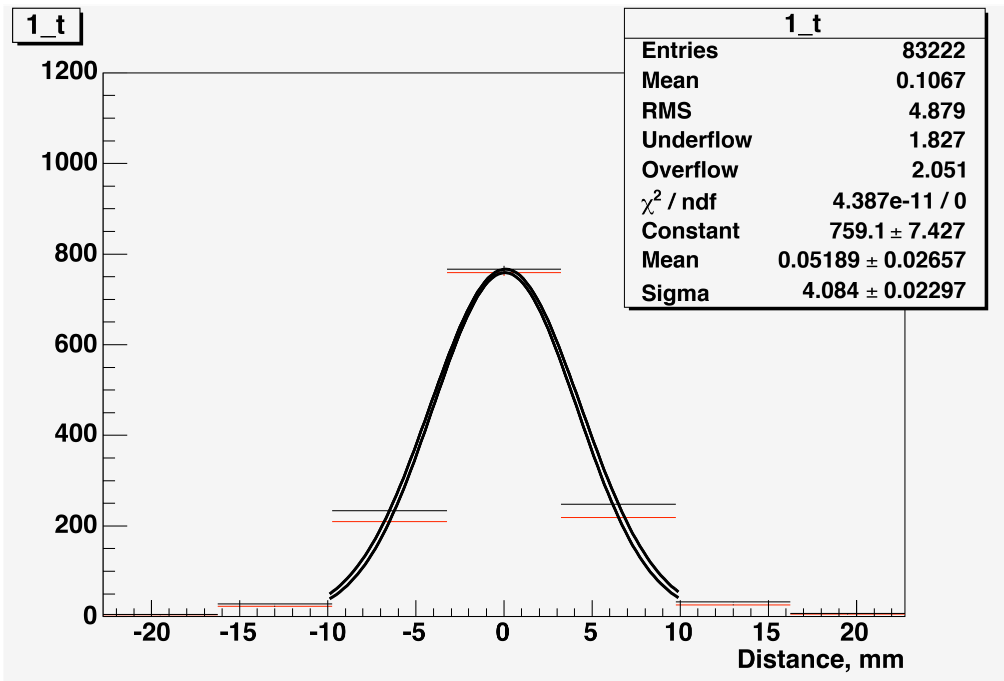

Figure 18: Average transverse charge profile of a single cluster in forward physics tracks, before (thick/black horizontal bars) and after (thin/red horizontal bars) correction for crosstalk, for all TPC sectors.

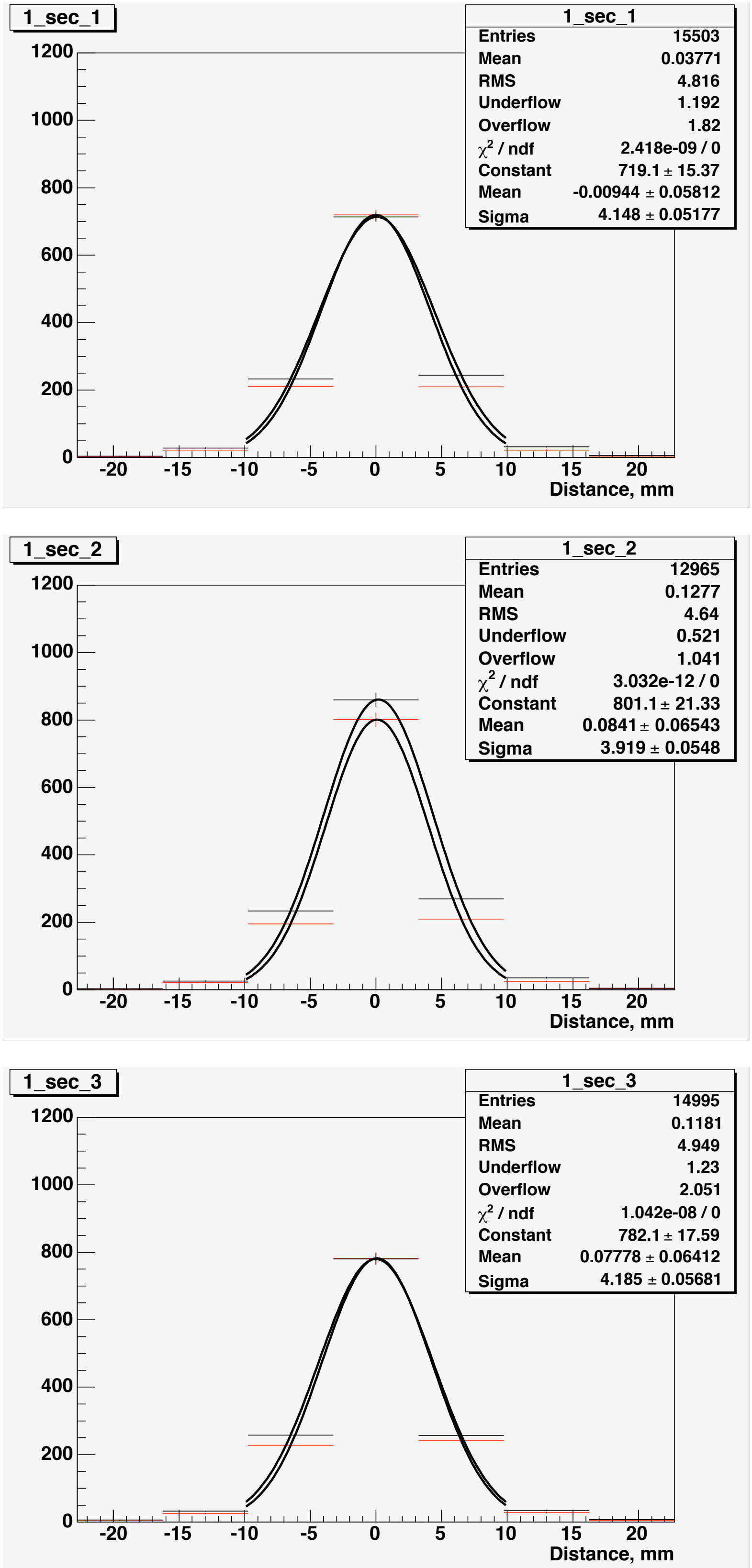

Figure 19: Average transverse charge profile of a single cluster in forward physics tracks, before (thick/black horizontal bars) and after (thin/red horizontal bars) correction for crosstalk, for TPC sectors 1 to 3.

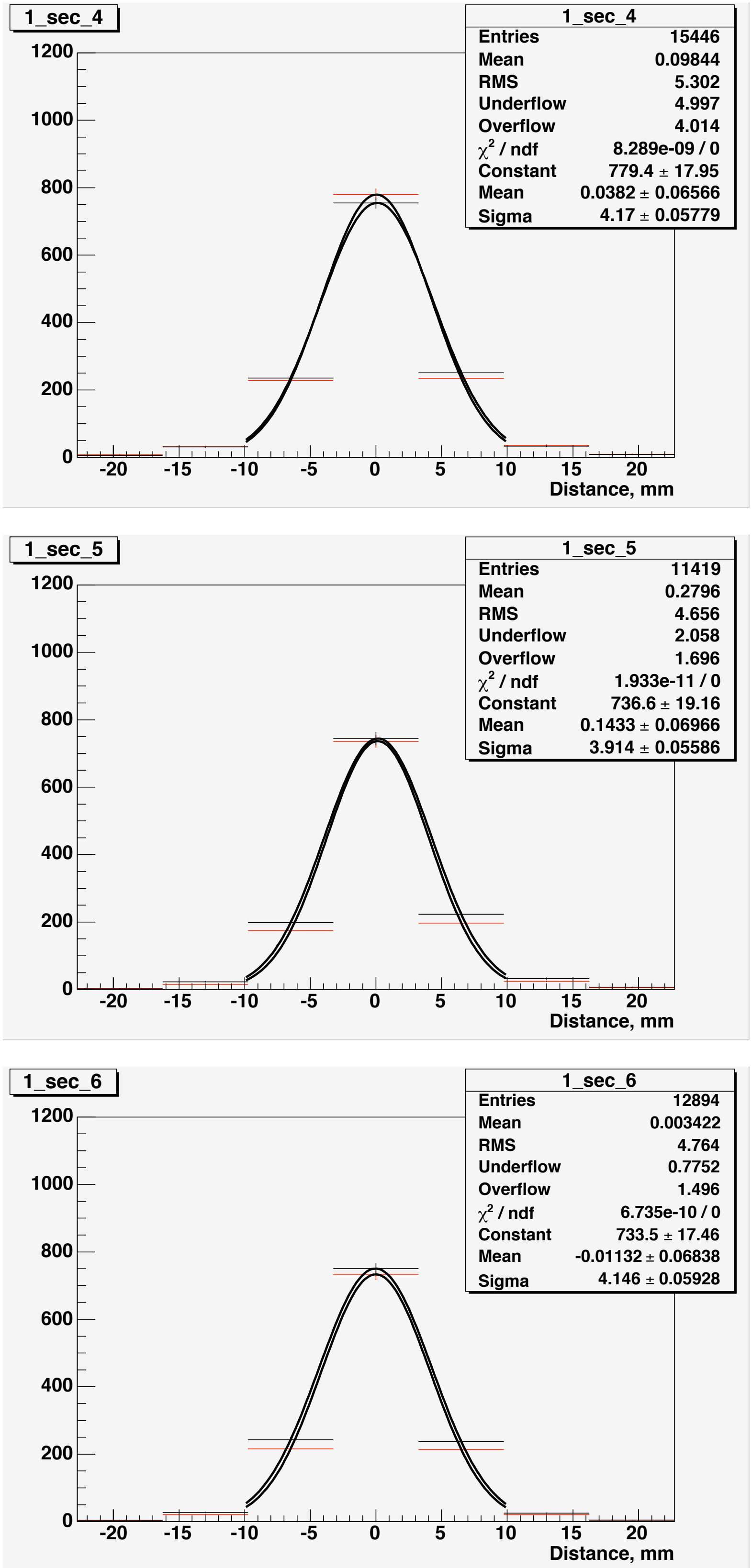

Figure 20: Average transverse charge profile of a single cluster in forward physics tracks, before (thick/black horizontal bars) and after (thin/red horizontal bars) correction for crosstalk, for TPC sectors 4 to 6.

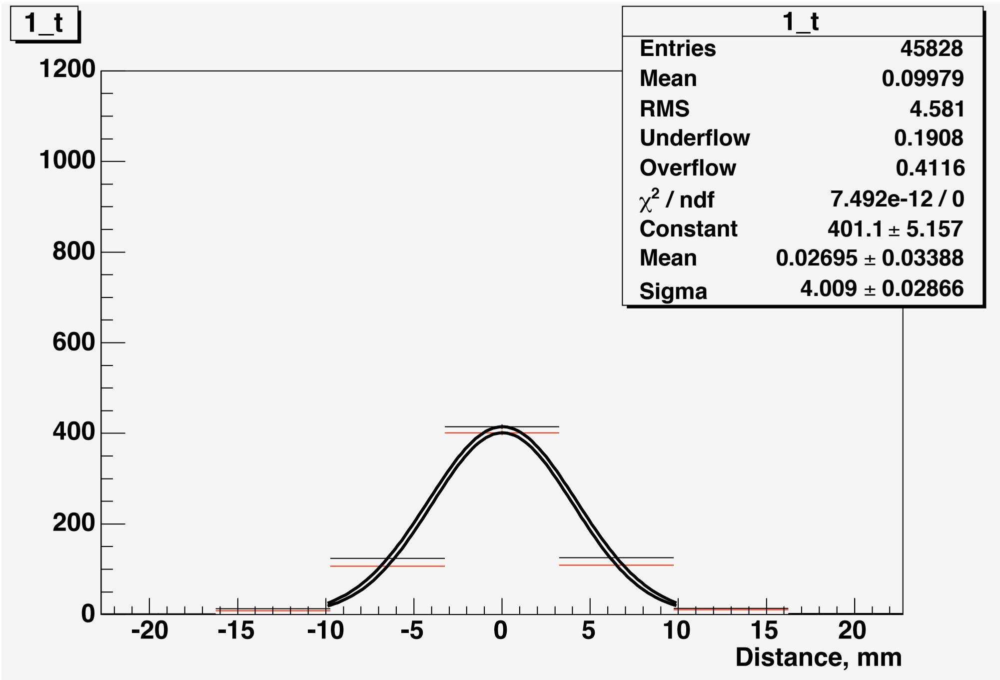

Figure 21: Average transverse charge profile of a single cluster in forward cosmic-muon tracks, before (thick/black horizontal bars) and after (thin/red horizontal bars) correction for crosstalk, for all TPC sectors.

References

[1] A. De Min *et al.*, TPC cross-talk correction: CERN–Dubna–Milano algorithm and results, HARP Memo 03-003, *http://cern.ch/dydak/crosstalk3.ps*

[2] A. De Min and F. Dydak, Analysis of HARP TPC krypton data, HARP Memo (submitted for internal publication), *http://cern.ch/dydak/kryptonCalib.ps*

[3] The ALEPH Handbook, Report ALEPH 89-77 (1989), editor W. Blum.

[4] J.C. Legrand, private communication.

[5] F. Dydak *et al.*, TPC track reconstruction: cluster positions and their errors, HARP Memo (in preparation).

[6] We thank R. Veenhof for useful discussions on the physics considerations behind the pad response function.

[7] J.S. Gordon and E. Mathieson, Nucl. Instr. Meth. **227** (1984) 267; E. Mathieson and J.S. Gordon, Nucl. Instr. Meth. **227** (1984) 277; and references cited therein.